J. Fluid Mech. (1970), *vol.* 43, *part* 2, *pp.* 269–277
Printed in Great Britain

The error minimization technique with application to a transonic nozzle solution

By ROBERT J. PROZAN AND DOUGLAS E. KOOKER
Aeromechanics Department, Lockheed Missiles and Space Company, Huntsville, Ala.

(Received 10 November 1969)

The error minimization technique is introduced as a method of obtaining the simultaneous solution to a set of partial differential equations. Because this numerical technique is at worst neutrally stable, it is believed to have fundamental advantages over existing techniques. The method is formulated in general for the steady fluid dynamic conservation equations and then applied to a specific case of irrotational isentropic flow of a perfect gas through a nozzle. Flow-field solutions were found in nozzle contours having a throat radius of curvature as low as 0·5. Comparison between experimental Mach number contours and the theoretical solution for a finite inlet nozzle with a conical exit is excellent.

Introduction

Numerical solutions to the partial differential equations of motion governing steady fluid flow have long been of interest. Basically, two methods have been advanced. They are: (i) asymptotic time-dependent solutions typified by Lax & Wendroff (1960, 1964), and (ii) relaxation techniques typified by the work of Emmons (1944, 1946). The asymptotic time-dependent method integrates the unsteady equations of motion forward in time. Introduction of a damping mechanism causes the process to converge to the steady-state solution. There are stability problems associated with this technique which preclude certain formulations and also affect the final closure on formulations which are otherwise acceptable (Armitage 1967). The relaxation methods are less formalized and success is often dependent on the skill, intuition and problem knowledge of the practitioner. To achieve a cyclic process which can reduce but not eliminate the largest residual before reducing the next largest residual has proved difficult. Although matrix inversion techniques can accomplish this, they become impractical for multi-variable multi-dimensional problems. The technique advanced here, which involves a relaxation process, is believed to have fundamental advantages over existing techniques.

General formulation

In their most general form, the conservation equations governing gaseous or fluid flow can be written

$$\frac{\partial w_k}{\partial t} = F^k\left(\mathbf{w}, \frac{\partial \mathbf{w}}{\partial x_i}, \frac{\partial^2 \mathbf{w}}{\partial x_i \partial x_j}, \ldots\right), \tag{1}$$

where $$\mathbf{w} = (w_1, w_2, \ldots, w_k, \ldots, w_K).$$

The w_k are the dependent fluid flow variables at a given point and the x_i are the spatial variables. For a fixed spatial grid system, using finite space derivatives, one may write

$$\frac{\partial w_k}{\partial t} = G^k(\mathbf{W}), \tag{2}$$

where $\mathbf{W}$ represents the dependent flow-field quantities over the entire field. The right-hand sides of (2) are simply non-linear algebraic functions of the flow variables, $\mathbf{W}$.

Since the steady-state solution is of interest, one may view the left-hand sides of (2) as errors or residuals which exist due to inaccurate knowledge of the flow variables, $\mathbf{W}$, influencing the point in question. Hence, let

$$\epsilon_k = G^k(\mathbf{W}). \tag{3}$$

Positive definite functions, P_k, of the error, ϵ_k, are used to define a local flow-field error at the point i as

$$g_i = \left[\sum_{k=1}^{K} P_k(\epsilon_k)\right]_i \tag{4}$$

such that g_i has the minimum value of zero when all the $\epsilon_k = 0$ at the i point. A merit function governing the entire flow field under investigation is defined by

$$g = \sum_{i=1}^{I} g_i, \tag{5}$$

where there are K equations in K unknowns governing each point in physical space and I grid points necessary to describe the region under investigation.

The result is a hypersurface g in $I \,.\, K$ unknowns. The problem becomes one of minimizing the function g by suitably adjusting the independent variables. Since the function is known and its gradient may be computed, a gradient technique seems most attractive as a means of performing the minimization. For the investigations described in this paper, a first-order scheme was used. Although more sophisticated techniques (Fletcher & Powell 1963) are available, there is no guarantee that the added complications are worth the effort for this type of problem.

From the calculus, $$dg = \nabla g \,.\, d\mathbf{W}, \tag{6}$$

where $$\mathbf{W} = W_1 \mathbf{i}_1 + W_2 \mathbf{i}_2 + \ldots + W_J \mathbf{i}_J,$$

$$\nabla g = \frac{\partial g}{\partial W_1} \mathbf{i}_1 + \frac{\partial g}{\partial W_2} \mathbf{i}_2 + \ldots + \frac{\partial g}{\partial W_J} \mathbf{i}_J.$$

The maximum change in g results (for a given $|d\mathbf{W}|$) when $d\mathbf{W}$ is parallel to ∇g. Thus

$$d\mathbf{W} = \frac{\nabla g}{|\nabla g|} |d\mathbf{W}|. \tag{7}$$

The desired change or payoff in g is

$$dg = g^{l+1} - g^l = -g^l, \tag{8}$$

where the index l denotes a point on the hypersurface g. Rewriting (6),

$$\mathbf{W}^{l+1} = \mathbf{W}^l - \left(\frac{g\nabla g}{|\nabla g|^2}\right)^l. \tag{9}$$

Equation (9) may be recognized as a multidimensional Newton–Raphson recursive formula and is generally referred to as steepest descent.

In arriving at the above relation, a first-order expansion is implied which will locate the desired solution in one step if the surface is a hyperplane. Further, it is reasonable to expect that the above recursion formula for a given step might increase the value of g, depending on the nature of the function. To eliminate this possibility, the length of the step is modified by introducing a multiplier on the correction term, i.e.

$$\mathbf{W}^{l+1} = \mathbf{W}^l - \left(\frac{g\nabla g}{|\nabla g|^2}\right)^l \delta. \tag{10}$$

Any time during the solution that $g^{l+1} > g^l$, the value of δ is reduced from its current value. Provisions for increasing δ may also be provided in the event that this is desired. Due to the control on δ, the above procedure is at worst neutrally stable. Moreover, the neutral stability condition can only occur when, in the limit as $\delta \to 0$, the gradient is incorrect due to computational inaccuracies or when a local minimum has been reached.

Transonic nozzle solution

In order to explore the economic feasibility of the method and to determine if local minima exist, the transonic flow field in an axisymmetric nozzle was chosen as an initial problem. The flow is assumed to be ideal, isentropic and isoenergetic. Under these conditions, only two equations and the point thermodynamic functions are required to completely specify the flow conditions at a point. The governing conservation equations are

$$\left.\begin{aligned} \epsilon_\rho &= \rho\left(\frac{\partial \tilde{u}}{\partial \tilde{x}} + \frac{\partial \tilde{v}}{\partial \tilde{r}} + \frac{\tilde{v}}{\tilde{r}}\right) + \tilde{u}\frac{\partial \rho}{\partial \tilde{x}} + \tilde{v}\frac{\partial \rho}{\partial \tilde{r}}, \\ \epsilon_s &= \frac{\partial \tilde{v}}{\partial \tilde{x}} - \frac{\partial \tilde{u}}{\partial \tilde{r}}, \end{aligned}\right\} \tag{11 a, b}$$

where $\tilde{u}$ and $\tilde{v}$ are the non-dimensional axial and radial velocities (scaled by a_0, the stagnation speed of sound), $\tilde{x}$ and $\tilde{r}$ are the axial and radial co-ordinates, ρ is the non-dimensional density scaled by the stagnation value of density ρ_0 and subscripts s and ρ indicate the momentum equation and continuity equation respectively. With the familiar relation of density as an isentropic function of velocity, the solution is dependent only on $\tilde{u}$ and $\tilde{v}$ for a given nozzle wall contour $R = R(\tilde{x})$.

Reasons of convenience, resolution and proper emphasis suggest the application of several transformations to these conservation equations. First, to achieve a centred orthogonal grid which includes the nozzle wall and the axis of symmetry as natural boundaries, let

$$r = \tilde{r}/R(\tilde{x}), \quad x = \tilde{x}. \tag{12}$$

One of the boundary conditions which must be satisfied at the nozzle wall, $r = 1$, demands that the velocity vector be parallel to the wall. An expedient way to ensure this is to transform $\tilde{v}$ as

$$\tilde{v} = Rv + \tilde{r}\beta\tilde{u}, \tag{13}$$

where

$$\beta \equiv \frac{dR}{d\tilde{x}} R.$$

Then, $v = 0$ when $r = 0$ and $r = 1$.

The flow field in the throat region of the nozzle is characterized by steep gradients and rapidly changing properties compared to the rest of the flow field. Thus, to emphasize the throat region while maintaining communication with the regions near the exit and entrance planes, let

$$x = K_1 \tan(\tfrac{1}{2}\pi\xi). \tag{14}$$

Redefining axial velocity,

$$\tilde{u} = \alpha u, \tag{15}$$

where

$$\alpha = dx/d\xi \quad \text{and} \quad u = d\xi/dt.$$

Equation (14) maps the interval $[-\infty \leqslant x \leqslant \infty]$ into $[-1 \leqslant \xi \leqslant 1]$ which will enable the one-dimensional velocity profile (normally assumed at some upstream station in a finite inlet area nozzle) to be moved to $x = -\infty$. In the throat region along the radial direction, the flow is changing much more rapidly near the nozzle wall than near the centre line. Thus, to emphasize the nozzle wall region while maintaining communication with the centreline region, let

$$r = \sin(\tfrac{1}{2}\pi\psi). \tag{16}$$

Redefining radial velocity

$$v = v^*/\omega, \tag{17}$$

where

$$v^* = d\psi/dt \quad \text{and} \quad \omega = d\psi/dr.$$

Thus, a uniformly space grid mesh system in the (ξ, ψ) plane places the proper emphasis on and lends accuracy to the rapidly changing regions in the physical $\tilde{x}$, $\tilde{r}$ plane.

The conservation equations (11) in terms of u, v^*, ξ and ψ become

$$\left.\begin{aligned} \epsilon_\rho &= \rho\left\{\frac{\partial u}{\partial \xi} + \kappa u + 2\alpha\beta u + \frac{v^*}{r\omega} + \left(\frac{\partial v^*}{\partial \psi} - v^*\lambda\right)\right\} \\ &\quad - \frac{u\rho}{\nu}\left[\alpha^2 u\left(\frac{\partial u}{\partial \xi} + \kappa u\right) + FF_{,\xi}\right] - \frac{v^*\rho}{\nu}\left[\alpha^2 u\frac{\partial u}{\partial \psi} + \frac{FF_{,r}}{\omega}\right], \\ \epsilon_s &= F_{,\xi} - \alpha\beta r F_{,r} - \frac{\alpha^2\omega}{R}\frac{\partial u}{\partial \psi}, \end{aligned}\right\} \tag{18a,b}$$

where

$$F \equiv Rv^*/\omega + \alpha\beta r R u,$$

$$F_{,\xi} = \frac{R}{\omega}\frac{\partial v^*}{\partial \xi} + \alpha\beta r R\left(\frac{\partial u}{\partial \xi} + \kappa u\right) + \alpha^2 r R u\beta' + \alpha^2\beta^2 r R u + \alpha R\beta v^*/\omega,$$

$$F_{,r} = R\left(\frac{\partial v^*}{\partial \psi} - v^*\lambda\right) + \alpha\beta R u + \alpha\beta r R\omega\frac{\partial u}{\partial \psi},$$

and $$\kappa = (d\alpha|d\xi)/\alpha, \quad \lambda = (d\omega|d\psi)/\omega, \quad \nu = 1-\tfrac{1}{2}(\gamma-1)(\tilde{u}^2+\tilde{v}^2),$$

where γ is the isentropic exponent, and $\beta' = d\beta/d\tilde{x}$.

A centred three-point differencing scheme was used to form a finite difference analogue for the partial derivatives. After substitution of these approximations for the derivatives into (18), the merit function, g, for this axisymmetric flow field was written

$$g = \sum_{i}^{I_0} \sum_{j}^{J_0} \{(\epsilon_\rho)_{ij}^2 + (\epsilon_s)_{ij}^2\}, \tag{19}$$

where I_0 and J_0 are the number of axial and radial grid points, respectively. Theoretically the choice of the positive definite functions is arbitrary. In practice, however, it is reasonable to expect that some functions will behave better, in the computational sense, than others. Equation (19) represents the definition used in this study and is not intended to infer that this is the only or even the best definition. Having made such a definition the components of the gradient of the hypersurface g can easily be computed by differentiating (19) with respect to each of the independent variables.

For the present application, the vector **W** in the general recursion relationship [equation (10)] is the sum of two independent vectors, **u** and **v***. Singling out one component of the **u** vector, the recursion relation for this i, j point becomes

$$u_{ij}^{l+1} = u_{ij}^{l} - \frac{g^l}{|\nabla g^l|^2}\left(\frac{\partial g^l}{\partial u_{ij}}\right)\delta. \tag{20}$$

An analogous expression can be written for v_{ij}^* components. The step on the error surface from l to $l+1$ is accomplished by first evaluating (20) for u_{ij} and its analogy for v_{ij}^* at every flow-field point. Then, all u's and v^*'s are simultaneously adjusted to their $l+1$ values, assuming δ was such that $g^{l+1} < g^l$.

The boundary conditions on the equations are imposed by use of the gradients of the error surface. Since the transformed radial velocity v^* is zero on the nozzle wall and centreline,

$$\left.\frac{\partial g^l}{\partial v^*}\right|_{\psi=1,0} = 0. \tag{21}$$

No explicit boundary condition exists for the axial component of velocity at $\psi = 1, 0$ in an inviscid analysis. The gradient of the error surface has a component $[dg^l/du]|_{\psi=1,0}$, but the solution proved to be sluggish and unresponsive when this was used as a boundary condition. Instead, the component $[dg^l/du]|_{\psi=1,0}$ was found from an extrapolation of the values at the two adjacent radial points. The value at the nozzle wall was a linear extrapolation of the two lower adjacent points and the centreline value was a symmetric extrapolation of the two upper adjacent points. Boundary conditions at the entrance and exit place were found from source and sink flow assumptions, respectively. These values were not altered as the solution progressed and therefore at $\xi = -1$ and $\xi = +1$

$$\frac{dg^l}{du} = \frac{dg^l}{dv^*} = 0. \tag{22}$$

Results

To demonstrate the capability of the method to handle flow fields in nozzle contours having a wide range of R_{tc}/R_t, where R_t is nozzle throat radius and R_{tc} the radius of curvature of nozzle contour in the throat, several runs were made with the axisymmetric hyperbolic contour,

$$R = [1 + b\tilde{x}^2]^{\frac{1}{2}}. \tag{23}$$

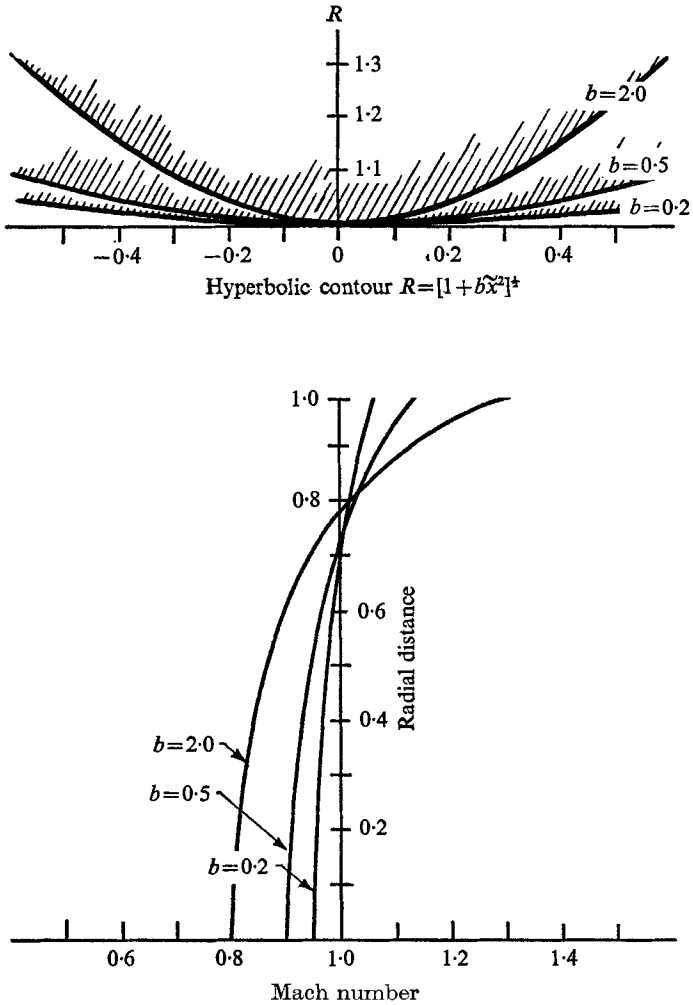

FIGURE 1. Mach number profile in physical throat for axisymmetric hyperbolic nozzle contours.

The three cases shown in figure 1 illustrate the Mach number profile in the physical throat for values of R_{tc}/R_t equal to 5·0, 2·0 and 0·5. These solutions were smooth and well behaved throughout the nozzle. The flow field was generated with 21 axial stations between $\xi = -1{\cdot}0$ and $+1{\cdot}0$ and 11 radial stations between

$\psi = 0$ and $+1{\cdot}0$. The even more extreme case of $R_{tc}/R_t = 0{\cdot}2$ has also been investigated but has shown the need for a greater number of mesh points and a longer time to relax to the final solution. The relaxation time may be reduced with a minimization technique more efficient than steepest descent.

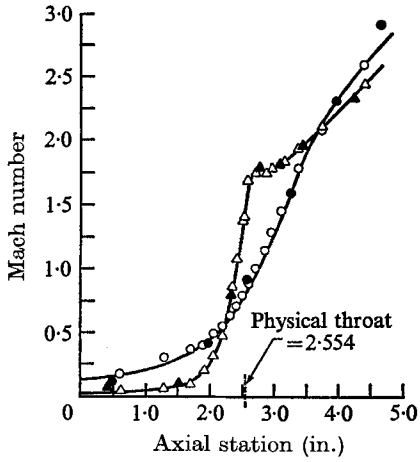

FIGURE 2. Comparison between error minimization solution and JPL data for nozzle wall and centreline Mach number distributions. ▲, nozzle wall measurement; △, nozzle wall prediction; ●, nozzle centreline measurement; ○, nozzle centreline prediction.

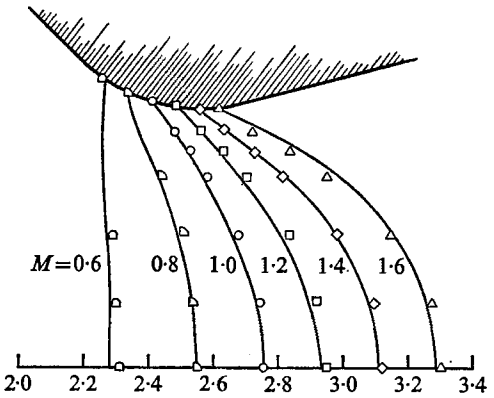

FIGURE 3. Comparison between experimental and theoretical Mach number contours in throat region of the JPL nozzle.

A nozzle contour with a finite area inlet and 15° conical exit using cold air as the flow medium has been analyzed experimentally by Jet Propulsion Laboratory (JPL) personnel. Back *et al.* (1965) and Cuffel *et al.* (1969) extensively surveyed the transonic region with probes and static pressure taps to determine the Mach number profiles. A theoretical analysis was made for this nozzle using the previous 231 gridpoint system and an assumption of uniform one-dimensional inlet flow at $\xi = -1{\cdot}0$. The resulting distributions of Mach number along the

nozzle wall and the centreline from this solution are compared to experimental data in figure 2. Figure 3 shows the comparison between six constant Mach contours determined from the analysis and the experimental survey data in the transonic region. The agreement is excellent. Typical run times on an IBM 7094 digital computer for these flow fields are between 5 and 10 min.

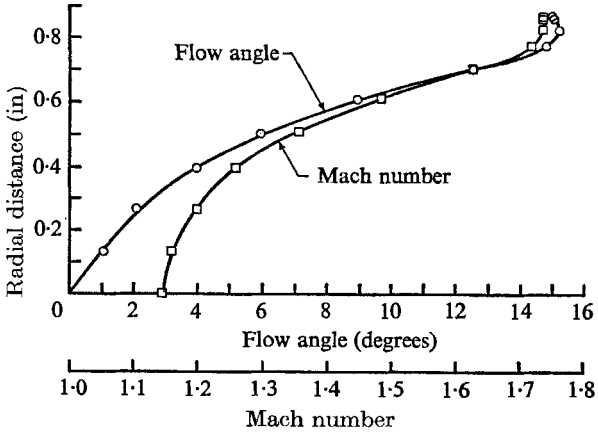

FIGURE 4. Theoretical Mach number and flow angle distribution in the JPL nozzle at axial station = 2·872.

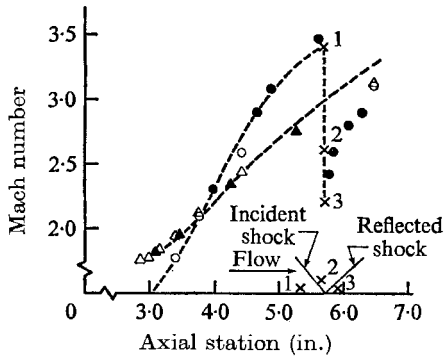

FIGURE 5. Mach number distribution on nozzle wall and centreline from method-of-characteristics as compared to the JPL data in the supersonic conical exit region. ▲, nozzle wall measurement; △, nozzle wall prediction; ●, nozzle centreline measurement; ○, nozzle centreline prediction; ----, method-of-characteristics solution.

One of the important uses of a transonic solution has been to provide accurate starting information for a method-of-characteristics solution in the supersonic region. A method-of-characteristics solution may be superior to any finite difference solution in this region because of its natural ability to treat shock waves as an interior boundary condition. Figure 4 presents a supersonic Mach number profile and the associated flow angle distribution for the $\xi = +0{\cdot}3$ station which was used as a 'start' line for the method of characteristics. In addition to the smooth Mach number distribution, the flow angle distribution

is exceptionally smooth, which is not necessarily characteristic of finite difference solutions. The results of this method-of-characteristics solution of the supersonic portion of the nozzle flow field are shown in figure 5. It can be seen that the predicted nozzle shock wave intersects the centreline at the location indicated by the experimental data.

Conclusions

A method to obtain the simultaneous solution of a set of partial differential equations, called the error minimization technique, was formulated in general and applied to the specific case of isentropic, irrotational flow of an ideal gas through a nozzle. The technique has several inherent and highly desirable advantages: (i) the relaxation process is, at worst, neutrally stable; (ii) until $\delta \to 0$, each step necessarily improves the overall solution; (iii) after the initial steps, the error is spread nearly uniformly over the entire flow field. The transonic flow-field analysis uncovered no local minima associated with the hypersurface, g.

Results obtained for the isentropic transonic flow problem are very encouraging. The solutions for axisymmetric hyperbolic contours with R_{tc}/R_t as low as 0·5 are smooth and well behaved. The solutions show excellent agreement with experimental data for a finite area inlet nozzle with a conical exit. The solution can provide smooth input data for a supersonic method-of-characteristics calculation. Some problems still remain in relaxing the end regions for severe nozzle contours, but a greater number of grid mesh points may eliminate this.

The error minimization technique has been shown to be a feasible method of solving complex mixed-flow problems in gas dynamics. Within the general formulation is the capability to solve the full Navier–Stokes equations for a viscous, heat-conducting fluid.

This work was supported by the NASA–Marshall Space Flight Center under Contract NAS 8-20082.

REFERENCES

ARMITAGE, J. V. 1967 *Aerospace Res. Labs., Wright–Patterson AFB.*
BACK, L. H., MASSIER, P. F. & GIER, H. L. 1965 *AIAA J.* **3**, 1614.
CUFFEL, R. F., BACK, L. H. & MASSIER, P. F. 1969 *AIAA J.* **7**, 1364.
EMMONS, H. W. 1944 *NACA TN* 932.
EMMONS, H. W. 1946 *NACA TN* 1003.
FLETCHER, R. & POWELL, M. J. D. 1963 *Computer J.* **6**, 168.
LAX, P. D. & WENDROFF, B. 1960 *Comm. Pure and Appl. Math.* **13**, **217**.
LAX, P. D. & WENDROFF, B. 1964 *Comm. Pure and Appl. Math.* **17**, 381.